ORIGINAL PAPER

Check for
updates

Broadside Coupled Split Ring Resonator as a Sensitive Tunable Sensor for Efficient Detection of Mechanical Vibrations

Sikha K. Simon[1] · Sreedevi P. Chakyar[1] · Anju Sebastian[1] · Jovia Jose[1,2] · Jolly Andrews[1] · V. P. Joseph[1]

Abstract

This paper explores the possibility of the precise determination of mechanical vibrations using metamaterial split ring resonator (SRR) structure. The amplitude of the interacting electromagnetic wave in the range of GHz frequency is directly varied in accordance with the amplitude of mechanical vibration, using a Broadside Coupled SRR (BCSRR) acting as a vibration sensor. Dependence of the spacing between the two rings on the resonance frequency of the BCSRR is used for the detection of vibration and it is achieved by allowing the spacing to change in accordance with the amplitude of mechanical vibration. For the effective sensing of mechanical vibration, the electromagnetic wave frequency is chosen at the center of the linear portion of the rising or the falling slope of the resonant curve of the BCSRR. By properly choosing the parameters of the BCSRR along with the effective tuning of the operating frequency, it is possible to detect even very weak vibrations. The chances of various distortions in the detected vibration waveform in connection with selection of the operating frequency and intensity of vibrations are also analyzed. The qualitative formulation of the detection process along with its experimental verification is presented. This novel method may find applications in the detection of mechanical vibrations caused by various man made and natural sources and may find manifold possibilities in the field of communication and instrumentation.

✉ V. P. Joseph
    vpj@christcollegeijk.edu.in

1   Department of Physics, Christ College (Autonomous), University of Calicut, Irinjalakuda, Kerala, India

2   Department of Physics, Vimala College (Autonomous), University of Calicut, Thrissur, Kerala, India

Springer

1 Introduction

Metamaterials, recently introduced artificially engineered materials, have evoked immense curiosity in scientific circles due to its unique characteristics and its potentiality for many phenomenal applications [5, 8, 24]. The rapid research in metamaterial inspired sensors have opened up new horizons in various fields of science and technology. The negative permeability inclusion of metamaterials called split ring resonators (SRR) usually place a major role in the development of different sensors [4, 10]. Sensors based on metamaterials are proved to be useful in different fields like material characterization, bio - medical applications, and in specific applications like vibration detection, food quality checking and identification of the changes in physical quantities like temperature, density and pressure [2, 11, 15–17, 21].

There were a few attempts, mostly in terahertz region, to modulate the resonant frequency by employing structural changes of the resonator or by incorporating some active electronic components in relation to some external physical parameters [3, 6, 9, 12, 19, 20, 22, 23]. Here we are introducing a method for detecting mechanical vibrations even of weak amplitude by employing a Broadside Coupled SRR (BCSRR) unit. The possibilities of changing the resonance frequency by varying the spacing between the two rings of the BCSRR in response to the amplitude of vibration in a controllable and sensitive way makes it an ideal candidate among different SRR structures for the proposed sensor [7, 13, 14]. The rings of the BCSRR used for the sensor are fabricated on two separate pieces of same substrate which helps to tune the spacing and the resulting capacitance of the resonator to any desired value. This BCSRR unit, capable of making vibrations of any of its rings in accordance with the mechanical vibration, attached to the microwave transmission system, the desired detection is achieved. The detailed qualitative formulation of the process along with various chances of distortions together with their experimental confirmation are presented. This novel proposal using BCSRR as a sensitive vibration sensor may find applications in fields like tunneling, piling, quarrying, seismic vibrational effects, usage of heavy machineries, hectic transportation etc where vibrational effects are dominant and in various fields of communication, instrumentation and surveillance.

2 Working of Sensor: A Qualitative Analysis

Conventional BCSRR consists of two co-axial rings on either sides of a single substrate of a low-loss material, where the splits of the rings are at diametrically opposite ends. For the proposed purpose of vibration sensor, the two metallic rings have to be arranged on two different pieces of substrate of the same material, so that it may have the capability of changing the spacing between the rings resulting in sensitive tuning of the resonance frequency. The resonance frequency of BCSRR depends on the inductance L and the capacitance C, which in this case varies in accordance with the spacing between the rings of the structure.

A possible resonance curve of a BCSRR structure for a particular spacing s is shown in Fig. 1a as a solid curve (reference curve) with resonance frequency f_0. The two dotted curves on either sides correspond to the resonance graphs for spacing slightly less (curve 2 with resonance frequency f_1) and slightly greater (curve 3 with resonance frequency f_2) than the initial spacing s. The qualitative formulation of the working of the vibration sensor is explained using the resonance curves of Fig. 1a as follows. We select a single frequency f_c on the linear portion either on the rising or the falling slope of the reference resonance curve (in this case, point A on the rising slope). If the resonance frequency of the BCSRR structure is slightly varied by changing the spacing between the rings, the absorption level corresponding to selected frequency f_c increases or decreases. If the changes in the spacing between the rings of the BCSRR is made in relation to the amplitude of mechanical vibration, the resonance frequency will also show a corresponding change. The curves 2 and 3 in Fig. 1a are two such typical cases. If the resonance frequency decreases from f_0 to f_1 (curve 2) due to decrease of the spacing, the power level for selected frequency f_c increases from point A to point B (equivalent to point B' of the reference curve). On the other hand, if the spacing increases the resonance curve shifts towards right (curve 3 with resonance frequency f_2) resulting in a reduced power level for f_c (point C, equivalent to point C' of the reference curve). Hence the power level variation of the selected frequency f_c is in co-relation with the strength of the mechanical vibration used for varying the spacing between the rings of the BCSRR. Thus we obtain a change in the microwave amplitude in accordance with the strength of the vibrating signal.

The graphical presentation of working process of vibration sensor is depicted in Fig. 1b. The spacing variation of the BCSRR rings s in accordance with the amplitude of mechanical vibration (input) is given in Fig. 1b-1. As the signal amplitude increases the spacing decreases and vice versa. The dependence of s on the resonance frequency is depicted in Fig. 1b-2. The capacitance C between the
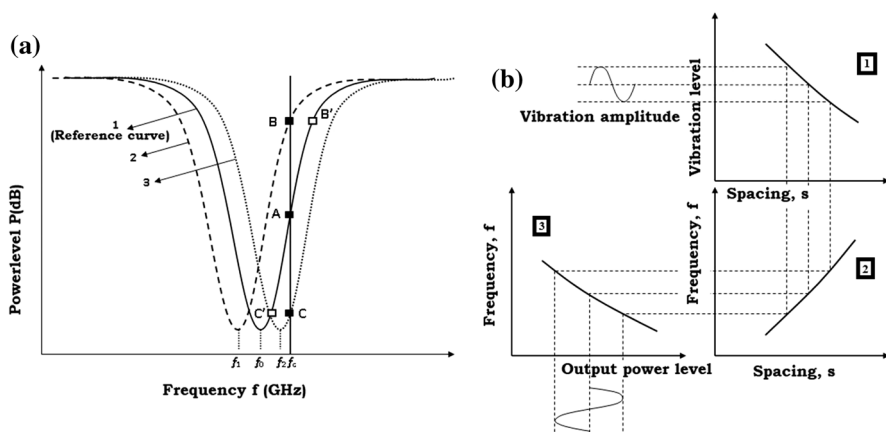

Fig. 1 **a** Possible resonance absorption curves of BCSRR for three different spacings (1—reference curve for spacing s, 2—curve for spacing less than s, 3—curve for spacing greater than s). **b** Graphical representation of the various stages involved in detection of mechanical vibration process

rings is inversely proportional to the spacing s and as C increases the resonance frequency f decreases based on the relation $f = 1/2\pi\sqrt{LC}$. The amplitude variation of the operating frequency f_c with changes in resonance frequency f is pictured in Fig. 1b-3. The maximum possible peak-to-peak value of the output power is the difference in power levels between points B and C as marked in Fig. 1a. The comparison of input and output wave forms shows that they are in phase.

If the operating frequency f_c is fixed at the center of the linear portion of the reference resonance curve (point A), for variation of power level between B and C, we will get the sensor output without any change in frequency or shape, detecting faithfully input vibration as shown in Fig. 2. If the amplitude level of the input signal causes the output power to exceed levels beyond B and C, it will result in distortion in the detected waveform as is shown in Fig. 3a and is explained as follows. As the frequency shifts towards left, the absorption level moves from A to B. For further shift of the resonance frequency beyond that, the absorption level remain fixed just above B resulting in a clipping at the positive half cycle of the output. On the other hand, as the resonance frequency shifts towards right, the output power level decreases to C. If there is further shift, the power level moves towards the minimum point of the resonance curve and then increases, resulting in a split in the output wave form. As the selection of the operating frequency moves towards B or C from the center point A, there are chances for different types of distortions in the output wave form. When the selected frequency is between A and B, distortion in the form of clipping happens in the positive half cycle only and is shown in Fig. 3b. Similarly, if the operating frequency is between A and C, positive half cycle is faithfully reproduced whereas the negative half cycle suffers a split as shown in Fig. 3c. When the operating point coincides with the resonance frequency dip of the reference absorption curve, both positive and negative half cycles of the input causes variation in absorption levels in a sinusoidal manner resulting in frequency doubling of the signal (Fig. 3d).
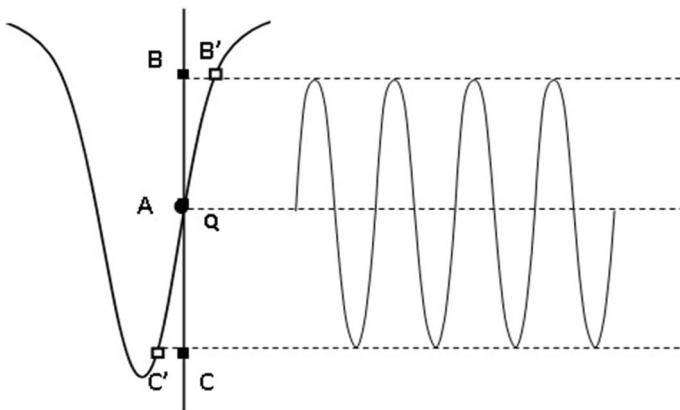

Fig. 2 Selection of the working frequency and the output power level variation for the faithful detection of a sinusoidal input vibration
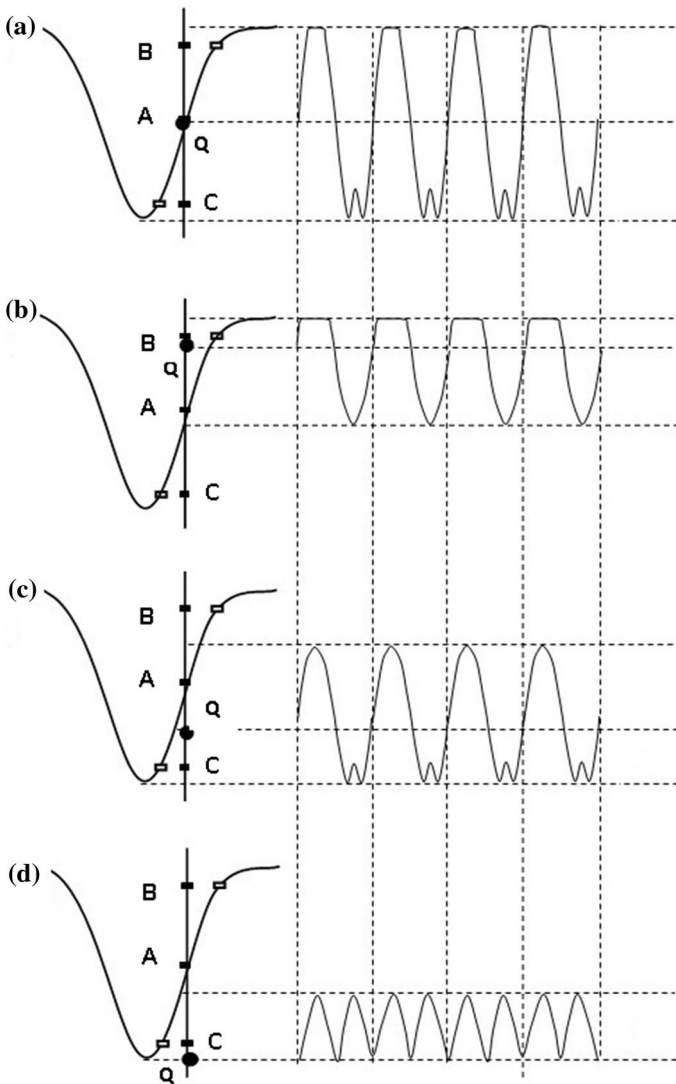
Fig. 3 The output wave forms for various types of distortion in relation to the intensity of the signal and the selection of the Q-points. **a** clipping due to intense input signal. **b–d** Distortions due to unexpected shifting of the Q-point

3 Experimental Confirmation and Results

The two rings of the BCSRR structure which are used for the experimental confirmation are fabricated by photochemical etching method on two pieces of FR4 circuit board (relative permittivity $\epsilon_r = 4.4$, thickness $t = 0.8$ mm) with inner radius $r = 2$ mm, width of the rings $c = 1$ mm and split width $d = 0.2$ mm [21]. For the verification of proposed vibration sensor technique, we need to properly attach the

sensor to any structure which undergoes vibration due to any reasons like mechanical tremor, ground vibrations etc. For the proper working of the sensor, the spacing between the rings of the BCSRR should change in relation to the input vibration.

In order to demonstrate the qualitative formulation of working of proposed vibration sensor including the various possibilities of errors in the vibration shape of detected signal, we have artificially generated a sinusoidal mechanical vibration using a electric signal with help of a transducer.

We have chosen a simple system of BCSRR unit cell attached to a speaker system (Fig. 4). One ring of the BCSRR is glued on a horizontal platform attached to the vibrating diaphragm of the speaker whereas the other is co-axially arranged just above it by attaching it to a rigid stand to set the BCSRR (Inset of Fig. 4 shows the rings of the BCSRR with spacing s). A sinusoidal audio signal from a function generator is given to the speaker which causes the speaker diaphragm to vibrate mechanically. The BCSRR is arranged between microwave transmitting (port 1) and receiving (port 2) probes connected to a Vector Network Analyzer (VNA) [1, 2, 18] and the setup is shown in Fig. 4. Before applying the signal from function generator the spacing between BCSRR rings is fixed at 1 mm and the corresponding reference resonance curve is plotted (Fig. 5) whose resonance frequency f_0 is 5.6 GHz.

The operating frequency f_c = 5.65 GHz is selected at the linear region of the rising slope of the resonance curve (equivalent to the point A of Fig. 1a) and the BCSRR is excited at this frequency. An input signal of frequency around 100 Hz and peak-to-peak voltage 0.5 V is directly fed to the speaker which causes vibrations of the speaker diaphragm resulting in a sinusoidal spacing variation of the BCSRR rings. Due to this, output power absorption level also varies sinusoidally with respect to A along the linear region (between B and C), giving an amplitude changes to the output wave and the displayed power level variation on the VNA screen is plotted in Fig. 6a. When the strength of the input signal increases beyond 1 V for the present transducer settings, distortion appears both on the upper and the lower portions due to excess amplitude of the vibration. The wave form obtained for this case is plotted in Fig. 6b-1. If the working
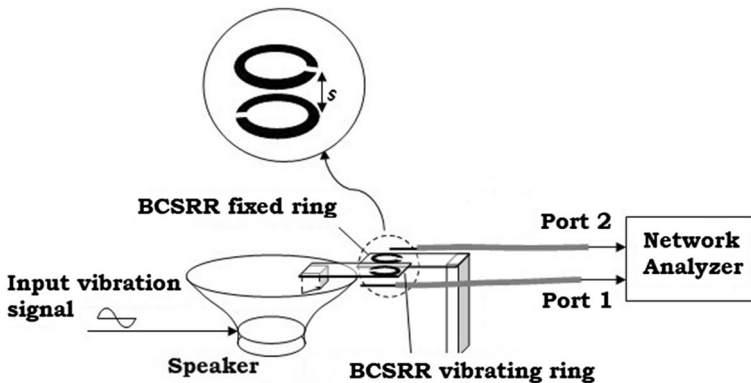

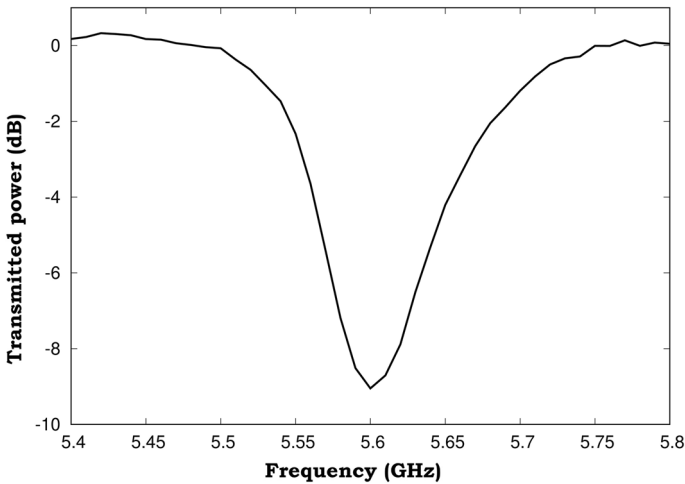**Fig. 4** Schematic representation of the experimental setup showing sensitive BCSRR vibration sensor and VNA

Fig. 5 Experimental transmission spectra of BCSRR used for the detection of mechanical vibrations

frequency is shifted to B (equivalent to point B'), we observe a positive clipping and it is shown in Fig. 6b-2. Similarly, a change in the operating frequency to a lower value C (equivalent to C') results in the output wave form to show distortion with splitting, which is shown in Fig. 6b-3. By choosing the operating frequency to exactly coincide with the resonance frequency of the reference curve, we obtain the doubling of the signal frequency which is given in Fig. 6b-4.

We have also demonstrated the mechanical vibrations caused by a freely falling standard weight (20 g from a height of 25 cm at a distance of 75 cm from the sensor probe) arranged on a wooden table of area 2 m^2 [21]. The experimental setup shown in Fig. 4 is used in this case also with slight modification. The speaker used for fixing one of the rings of the BCSRR is replaced with a sensitive cantilever arrangement. A steel bar of length 15 cm, breadth 2 cm and thickness 0.75 mm is mounted on a wooden base to form the cantilever with the BCSRR ring attached to its free end. The corresponding output vibration patterns are depicted in Fig. 7. Figure 7a depicts vibration when the operating frequency is around the center portion of rising slope of resonance curve (point A) which is a sinusoidal damped waveform. Figure 7b shows distortion in the output vibration signal due to the shifting of operating frequency towards the topmost point of the resonance curve (point B). The output power level of the sensor not only depends upon the amplitude of the mechanical vibration but also on the sensitiveness of the BCSRR arrangement. Even for very weak vibrations, by choosing a sensitive arrangement, significant changes in the resonance frequency can be obtained which provides feasible chances for enhanced detection of vibrational levels. Alternatively, choosing a BCSRR with sharp resonance band width also results in sensitive detection of very weak signals.
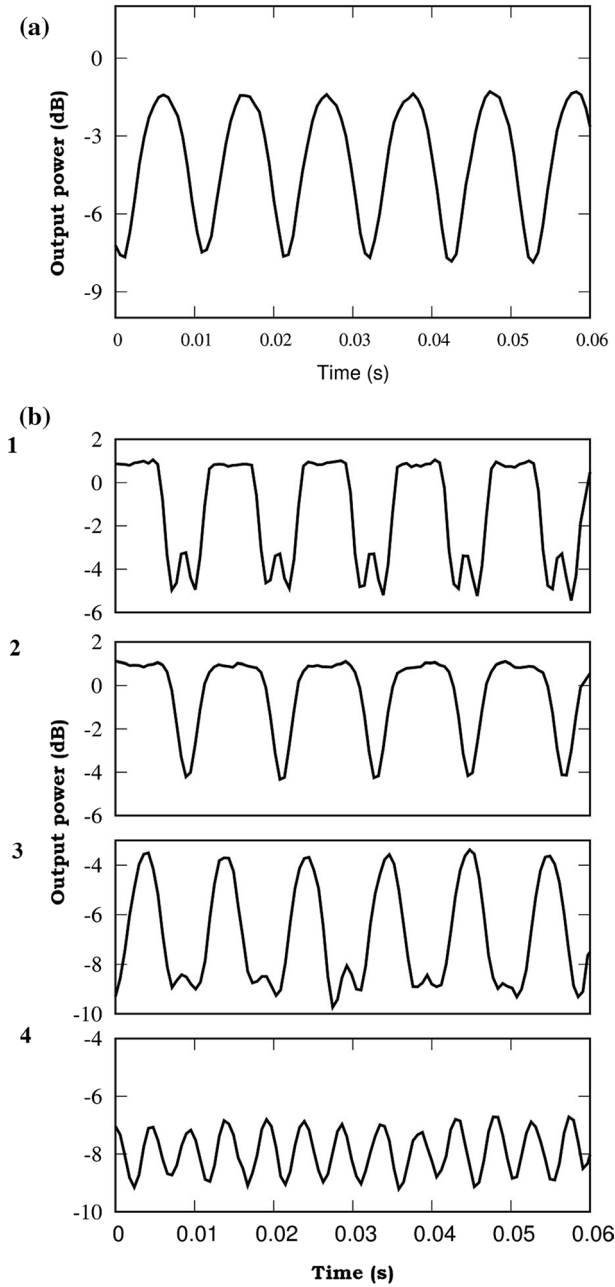
Fig. 6 Experimental plot of power variation obtained for **a** faithful detection, **b** errors during detection
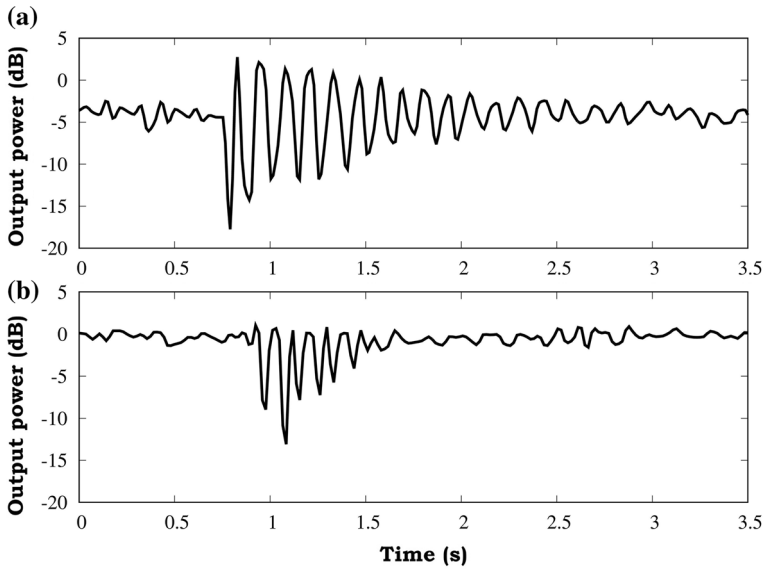
(a)

(b)

Fig. 7 **a** Output vibration pattern due to a freely falling standard weight of 20 g. **b** Distortions in the output due to shifting of operating frequency

4 Conclusions

In this work we have introduced metamaterial BCSRR as a sensitive tunable sensor for efficient detection of mechanical vibrations. A qualitative analysis of the working of the sensor is presented along with sufficient experimental support. Various chances of distortions are also analyzed with respect to the strength of the input vibration signal and selection of the working frequency in relation to the resonance frequency of the BCSRR. Our novel sensor can be effectively used in the sensitive detection of mechanical vibrations caused by various man made sources such as tunneling, pilling,quarrying etc and vibrations caused by seismic effects. This may find applications in the field of communication and in different control systems. It can also be used for the effective tuning of the output power level of microwaves with the help of a weak control voltage and in the development of microwave instrumentation which employs metamaterial as a control element.

References

1. Aydin, K., Bulu, I., Guven, K., Kafesaki, M., Soukoulis, C. M., & Ozbay, E. (2005). Investigation of magnetic resonances for different split-ring resonator parameters and designs. *New journal of physics*, *7*(1), 168.
2. Chakyar, S. P., Simon, S. K., Bindu, C., Andrews, J., & Joseph, V. P. (2017). Complex permittivity measurement using metamaterial split ring resonators. *Journal of Applied Physics*, *121*(5), 054,101.
3. Chen, H. T., Padilla, W. J., Cich, M. J., Azad, A. K., Averitt, R. D., & Taylor, A. J. (2009). A metamaterial solid-state terahertz phase modulator. *Nature photonics*, *3*(3), 148–151.
4. Chen, T., Li, S., & Sun, H. (2012). Metamaterials application in sensing. *Sensors*, *12*(3), 2742–2765.
5. Cui, T. J., Smith, D. R., & Liu, R. (2014). *Metamaterials*, (Vol. 3). Berlin: Springer.
6. Degiron, A., Mock, J. J., & Smith, D. R. (2007). Modulating and tuning the response of metamaterials at the unit cell level. *Optics express*, *15*(3), 1115–1127.
7. Ekmekci, E., & Turhan-Sayan, G. (2013). Multi-functional metamaterial sensor based on a broad-side coupled srr topology with a multi-layer substrate. *Applied Physics A*, *110*(1), 189–197.
8. Engheta, N., & Ziolkowski, R. W. (2006). Metamaterials: physics and engineering exploration. Hoboken: John Wiley & Sons.
9. Fan, Y., Qiao, T., Zhang, F., Fu, Q., Dong, J., Kong, B., & Li, H. (2017). An electromagnetic modulator based on electrically controllable metamaterial analogue to electromagnetically induced transparency. Scientific Reports 7.
10. Jeppesen, C. (2010). Metamaterials for sensing applications. PhD thesis, Technical University of DenmarkDanmarks Tekniske Universitet, Department of Photonics EngineeringInstitut for Fotonik, NanophotonicsNanofotonik.
11. Kairm, H., Delfin, D., Shuvo, M. A. I., Chavez, L. A., Garcia, C. R., Barton, J. H., et al. (2015). Concept and model of a metamaterial-based passive wireless temperature sensor for harsh environment applications. *IEEE Sensors Journal*, *15*(3), 1445–1452.
12. Lahiri, B., Khokhar, A. Z., Richard, M., McMeekin, S. G., & Johnson, N. P. (2009). Asymmetric split ring resonators for optical sensing of organic materials. *Optics express*, *17*(2), 1107–1115.
13. Marqués, R., Medina, F., & Rafii-El-Idrissi, R. (2002). Role of bianisotropy in negative permeability and left-handed metamaterials. *Physical Review B*, *65*(14), 144,440.
14. Marqués, R., Mesa, F., Martel, J., & Medina, F. (2003). Comparative analysis of edge-and broadside-coupled split ring resonators for metamaterial design-theory and experiments. *IEEE Transactions on Antennas and Propagation*, *51*(10), 2572–2581.
15. Melik, R., Unal, E., Kosku Perkgoz, N., Puttlitz, C., & Demir, H. V. (2009a). Flexible metamaterials for wireless strain sensing. *Applied Physics Letters*, *95*(18), 181,105.
16. Melik, R., Unal, E., Perkgoz, N. K., Puttlitz, C., & Demir, H. V. (2009b). Metamaterial-based wireless strain sensors. *Applied Physics Letters*, *95*(1), 011,106.
17. Raghavan, S., & Rajeshkumar, V. (2013). An overview of metamaterials in biomedical applications. *Session 2A8*, *245*, 25–28.
18. Ragi, P. M., Umadevi, K., Nees, P., Jose, J., Keerthy, M., & Joseph, V. (2012). Flexible split-ring resonator metamaterial structure at microwave frequencies. *Microwave and Optical Technology Letters*, *54*(6), 1415–1416.
19. Rao, S. J. M., Kumar, D., Kumar, G., & Chowdhury, D. R. (2017). Modulating the near field coupling through resonator displacement in planar terahertz metamaterials. *Journal of Infrared, Millimeter, and Terahertz Waves*, *38*(1), 124–134.
20. Shrekenhamer, D., Rout, S., Strikwerda, A. C., Bingham, C., Averitt, R. D., Sonkusale, S., et al. (2011). High speed terahertz modulation from metamaterials with embedded high electron mobility transistors. *Optics express*, *19*(10), 9968–9975.
21. Sikha, Simon K., Chakyar, SP., Andrews, J., & Joseph, VP. (2017). Metamaterial split ring resonator as a sensitive mechanical vibration sensor. In American Institute of Physics Conference Series, vol 1849.
22. Singh, R., Al-Naib, I. A., Koch, M., & Zhang, W. (2011). Sharp fano resonances in thz metamaterials. *Optics express*, *19*(7), 6312–6319.

23. Yang, Y., Huang, R., Cong, L., Zhu, Z., Gu, J., Tian, Z., et al. (2011). Modulating the funda-
     mental inductive-capacitive resonance in asymmetric double-split ring terahertz metamaterials.
     Applied Physics Letters, *98*(12), 121,114.
24. Zheludev, N. I., & Kivshar, Y. S. (2012). From metamaterials to metadevices. *Nature materials*,
     11(11), 917–924.